Journal Pre-proof



Probing rare Von Willebrand's Disease causing mutations in the D4 and C-domains of Von Willebrand Factor.

Golzar Mobayen, Sammy El-Mansi, Alain Chion, Thomas D. Nightingale, Thomas A.J. McKinnon

PII: S2475-0379(25)00246-8

DOI: https://doi.org/10.1016/j.rpth.2025.102922

Reference: RPTH 102922

To appear in: *Research and Practice in Thrombosis and Haemostasis*

Received Date: 4 May 2025

Accepted Date: 2 June 2025

Please cite this article as: Mobayen G, El-Mansi S, Chion A, Nightingale TD, McKinnon TAJ, Probing rare Von Willebrand's Disease causing mutations in the D4 and C-domains of Von Willebrand Factor., *Research and Practice in Thrombosis and Haemostasis* (2025), doi: https://doi.org/10.1016/j.rpth.2025.102922.

This is a PDF file of an article that has undergone enhancements after acceptance, such as the addition of a cover page and metadata, and formatting for readability, but it is not yet the definitive version of record. This version will undergo additional copyediting, typesetting and review before it is published in its final form, but we are providing this version to give early visibility of the article. Please note that, during the production process, errors may be discovered which could affect the content, and all legal disclaimers that apply to the journal pertain.

© 2025 The Author(s). Published by Elsevier Inc. on behalf of International Society on Thrombosis and Haemostasis.

Journal Pre-proof

Probing rare Von Willebrand's Disease causing mutations in the D4 and C-domains of Von Willebrand Factor.

Golzar Mobayen[1‡], Sammy El-Mansi[2], Alain Chion[3], Thomas D. Nightingale[2] and Thomas A.J. McKinnon[1‡]

[1]Deparment of Immunology and Inflammation, Centre for Haematology, Imperial College Academic Health Science Centre, Hammersmith Hospital, London W12 0NN, United Kingdom.

[2]Centre for Microvascular Research, William Harvey Research Institute, Faculty of Medicine and Dentistry, Queen Mary University of London, London, United Kingdom

[3]Irish Centre for Vascular Biology, School of Pharmacy and Biomolecular Sciences, Royal College of Surgeons in Ireland, Dublin, Ireland.

‡ to whom correspondence should be addressed

Email: t.mckinnon03@imperial.ac.uk and golzar.mobayen17@imperial.ac.uk

Running title: VWD variants in the C-terminal domains of VWF

Key words: Von Willebrand Factor, Von Willebrand's disease, variant analysis, bleeding

Abstract word count: 248

Text word count: 4514

No. of figures: 6

No. of tables: 2

Journal Pre-proof

Journal Pre-proof

Abstract

Background

Von Willebrand's Disease is characterised by an absence or reduction of plasma Von Willebrand Factor levels or reduced protein function. While the spectrum of causative Von Willebrand's Disease (VWD) mutations is vast, there has been limited characterisation of variants occurring within the D4-C6 domains of VWF that comprise the C-terminal portion of the molecule.

Objectives

In the present study we investigated the impact of nine putative low frequency VWD causing variants on VWF function.

Methods

Variants were generated by site directed mutagenesis and expressed in HEK293(T) cells and analysed for expression, intracellular storage and multimeric profile. The ability of Arg2379Cys to form dimers was assessed using an A2-CK fragment of VWF.

Results

Arg2379Cys, Ser2497Pro and Cys2639Tyr had significantly reduced secretion from HEK293T cells, while the other mutations all failed to be secreted. While co-transfection with wtVWF appeared to rescue expression, co-transfection with a deletion A1 construct demonstrated that only the Gly2044Asp, Glu2343Val, Ser2497Pro and Cys2693Tyr variants could be rescued. All the variants failed to form appreciable pseudo-Webiel-Palade bodies in HEK293 cells and showed abnormal multimers in cell lysates. The Arg2379Cys variant could be overexpressed by only formed monomers and some dimers. Analysis with a VWF-A2CK protein demonstrated that in the homozygous state Arg2379Cys behaves likes a type 2A variant, while it is likely to be a type 1 variant in the heterozygous state.

Conclusion

This data shows that varaints within the C-terminal region of VWF can dramatically impact proper VWF expression and can different impacts on VWF depending on homo or heterozygosity.

Journal Pre-proof

Journal Pre-proof

Background

Von Willebrand Factor (VWF) is a large plasma glycoprotein essential to normal haemostasis by acting as the carrier molecule for coagulation factor VIII and supporting platelet adhesion and aggregation at sites of vascular injury.[1, 2] VWF is synthesised exclusively in endothelial cells and megakaryocytes where it is stored in Weibel-Palade bodies and α-granules respectively.[3, 4] Critical to its function is its multimeric size, with the largest multimers being the most active.[5] VWF monomers are comprised of a series of repeating domains arranged in the order: D1D2-D'D3-A1A2A3-D4C1C2C3C4C5C6CK with many of the domains having functional characterised roles.[6] The D1D2 domains comprise the propeptide and are essential for multimer formation;[7] the cysteine knot (CK) domains contains cysteines residues required for dimer formation;[8] the D'D3 domain contain the FVIII binding sites and cysteine residues required for multimer formation.[9-11] The A1 and A3 domains bind to exposed collagen and the A1 domain interacts with platelet glycoprotein (GP) Ibα.[12-15] The A2 domain harbours the A Disintegrin And Metalloprotease with ThromboSpondin motif repeats 13 (ADAMTS13) cleavage site, with a docking site for ADAMTS13 reported in the D4 domain.[16, 17] Finally the C4 domain presents an RGD sequence required for binding to platelet GPIIb/IIIa.[18]

The clinical importance of VWF is highlighted by Von Willebrand Disease (VWD) which is generally caused by mutations in the *VWF* gene and is characterised by a bleeding phenotype which can vary in severity from asymptomatic to life-threatening bleeding.[19, 20] VWD is the result of either a quantitative or qualitative deficiency of VWF and can be broken down into three subtypes. Type 3 VWD is characterised by a total absence of VWF in the circulation, whereas type 1 represents reduced plasma levels. It is noteworthy that a small portion of type 1 patients do not have a mutation in the VWF gene.[21] Type 2 VWD is broken down into further subtypes and results from functional defects such as aberrant multimer formation (Type 2A – group I), enhanced susceptibility to ADAMTS13 cleavage (Type 2A – group II), reduced collagen or platelet binding (Type 2M), enhanced binding to GPIbα leading to increased proteolysis and clearance (Type 2B) and reduced FVIII binding (Type 2N)[19].

The spectrum of missense VWD causing variants is vast with mutations reported in every domain. While many of these are rare variants and often only appear in the heterozygous state, knowing where the mutation occurs can be useful for diagnosis and clinical management however genetic testing is not performed for the majority of cases. [22] Studies reporting on the phenotypical effects of variants on VWF expression and function using recombinant expression and *in vivo* systems provide significant information about the impact of the variant. Regardless of the frequency of a particular variant, such

studies enhance our understanding of VWF biology and can in some cases help to guide the appropriate treatment.[23-31] However many reports tend to focus on VWD causative variants in the N-terminal portion of the molecule, taken as the D1 to A3 domains with much less attention paid to the C-terminal region; D4 – CK and indeed our overall understanding of how this part of VWF functions is under explored compared to the N-terminal domains. Although recently Dubois et al described two frame shift variants located in the D4 domain. [32]

To address this, in the present study we selected rare 9 putative missense variants in the D4 and C1-C6 domains that are associated with VWD but have yet to been extensively characterised using *in vitro* studies. Using a recombinant expression system, we demonstrate that variants in the D4 and C-domains of VWF can significantly affect VWF expression and function and the impact of the causative mutation can be different depending on its hetero or homozygous status.

Journal Pre-proof

Journal Pre-proof

Methods

Variant selection

The gnomAD v4.1.0 database[33] was accessed via https://gnomad.broadinstitute.org/ and a search performed for "VWF" to show only "missense/inframe indel" variants and data was saved as a CSV file. Variants falling outside the D4 to C6 domains (taken as residues 1873-2722) were discarded along with inframe and indel variants, leaving only missense mutations. Variants were selected at random and cross-referenced to the EAHAD coagulation factor variant database to determine if any clinical data was available and if any *in vitro* functional work had been performed. Additionally basic literature searches were carried out using Pubmed and Google, searching for the mutant location with either single or triple letter amino acid code and either "VWF" or "VWD". Variants that had previously *in vitro* characterisation were excluded.

Expression of VWF mutants

Full length VWF mutants were generated as previously described. Mutagenesis primers were designed using Primer X (https://www.bioinformatics.org/primerx/) and the QuikChange XL site-directed mutagenesis kit (Stratagene) was used to generate mutations in the vector pcDNA3.1-VWF-A2CK which encodes for the VWF A2 through to CK domain. Following confirmation of the desired mutation the A2-CK fragments was sub-cloned into our full length VWF expression vector pcDNA3.1-FL-VWF using the restriction enzymes KpnI and AgeI. All mutations were reconfirmed by DNA sequencing. Wild type (wt) and mutated VWF were then expressed in HEK293T cells as previously reported using 10mM polyethylenimine (PEI) as a transfection reagent. Three days post-transfection the conditioned medium was collected and cells were lysed in chilled lysis buffer (150mM NaCl, 50mM Tris, 5mM EDTA 1% Triton 100x pH7.4) for 5 minutes on ice. Lysates were then collected and centrifuged at maximum speed (13,500rpm) for 10 minutes to remove cellular debris. For large scale protein production the conditioned media was concentrated ~20-fold using 100kDa Amicon Ultra 15ml centrifugation filter units (Millipore, UK). For co-transfection experiments, HEK293T cells were transfected with the mutated VWF sequences alongside either pcDNA3.1-FL-VWF or the vector pcDNA3.1-FL-VWF-ΔA1 construct that lacks the A1 domain in a 1:1 ratio.[34, 35]

Immunofluorescence analysis of intracellular VWF

Immunofluorescence analysis of intracellular VWF was performed using HEK293 cells since HEK293T cells fail to form WPB-like granules. HEK293 cells expressing WT and mutant VWF constructs were

fixed with 4% para-formaldehyde for 15 minutes in the dark. The fixed cells were washed three times with PBS and then permeabilised by the addition of 1% Triton (Sigma, UK) diluted in PBS for 10 minutes at room temperature. Cell were subsequently washed and stained for VWF and the Endoplasmic Reticulum (ER) using sheep polyclonal anti-Von Willebrand Factor antibody (FITC) (CiteAb, UK) and mouse anti-PDI Antibody (F-4) (Santa Cruz Biotechnology, USA) both diluted to 1µg/ml, for 1 hour at room temperature. Following staining cells were washed 4 times with PBS and then stained with goat anti-mouse AlexaFluor-555 secondary antibody diluted 1 in 2000 for 20 mins. After washing, coverslips were mounted on glass slides using mounting medium with 4',6-diamidino-2-phenylindole (DAPI) (Abcam, UK). Images were acquired using the Zeiss LSM800 confocal microscope. Images are presented as a maximum intensity projection of 0.5µm interval Z stacks.

Protein analysis

VWF levels in the media and lysate were quantified using an "in-house" VWF ELISA and multimers distribution of VWF in the media and lysate was assessed using non-reducing 1.2% agarose gel electrophoresis both as previously described.[36, 37] Analysis of the VWF A2-CK protein was performed using sodium dodecyl sulphate polyacrylamide gel electrophoresis (SDS-PAGE). Samples were diluted with NuPAGE™ LDS Sample Buffer (4X) (Invitrogen, UK) supplemented with 7% β-mercaptoethanol (Sigma, UK) as a reducing agent when required. Precast 4-12% Bis-Tris Gels (Invitrogen, ThermoFisher Scientific, UK) were set up in Mini Gel Tanks (Invitrogen, ThermoFisher Scientific, UK) with 1x NuPAGE MES SDS Running buffer (Invitrogen, ThermoFisher Scientific, UK). Samples were denatured for 10 minutes at 90°C, and then loaded onto the gel alongside a pre-stained 10-250kDa marker (Cell signalling, USA). Electrophoresis was carried at 200V for ~40 minutes. Following SDS-PAGE, proteins were transferred onto nitrocellulose membranes using the Bio-Rad Trans-Blot Turbo Transfer System (BioRad, UK) following manufacturer protocol using the high molecular weight programme for 15 minutes. Membranes were then blocked in PBS supplemented with 0.1% Tween-20 (PBS-T) containing 2% skimmed milk (Sigma, UK) on a roller for 1 hour at room temperature. Following blocking, membranes were incubated with polyclonal anti-VWF-HRP (Dako, UK) conjugated antibodies to detect VWF-A2-CK.Protein was detected using SuperSignal West Pico Plus Chemiluminescence substrate (ThermoFisher, Scientific, UK) and membranes visualised using the iBright 1500 Imaging system (ThermoFisher, Scientific, UK).

Perfusion assays

Analysis of VWF function under flow was carried out essentially as previously described.[24] In brief, Ibidi $VI^{0.1}$ slides were coated with 100µg/ml human type III collagen (Southern Biosciences) overnight

Journal Pre-proof

in a humidified chamber. Channels were washed three times with PBS before the addition of 2% BSA/PBS for a minimum of 15 minutes. Plasma free blood (PFB) was prepared as previously described, with platelets rendered fluorescent by the addition of 10mM $DiOC_6$ (3,3'-Dihexyloxacarbocyanine iodide) (ThermoFisher Scientific, UK). The PFB was supplemented with 2.5 µg/ml of either wild-type or mutant VWF and perfused over the collagen surface at 140 µl/min to give a final wall shear rate of $1500s^{-1}$. Images of bound platelets were captured in real-time under an Olympus-CKX41 inverted fluorescent microscope linked to a Rollera XR camera. Platelet capture was analysed using ImageJ software.

Structural models

Since there is no experimental structure for the VWF D4-C6 region, we used the Alphafold model for porcine VWF (AF_AFQ28833F1; https://www.rcsb.org/structure/AF_AFQ28833F1) as a template for modelling with Modeller software. [38] The porcine VWF Alphafold model is better than the human VWF Alphafold model in A3-CK region. A VWF-A3-C3 model (residues 1672-2496) and a VWF-C1-C6 model (residues 2256-2720) were generated and analysed using Pymol software.

Data Analysis

Data analysis was performed using Prism Software for Science software package (version 10.0, GraphPad Software). Results are expressed as SD with mean. The statistical significance of differences between groups was assessed using one-way ANOVA with multiple comparisons.

Journal Pre-proof

Journal Pre-proof

Results

The spectrum of D4 and C-domains missense variants

The D4 and C-domains of VWF comprise residues 1873 – 2722 and are encoded by exons 35 to 50 of the *VWF* gene. We initially interrogated the gnomAD database and found 1041 reported missense variants between amino acids 1873 to 2722 inclusive; representing mutation of 623/850 (73.1%) of the amino acids comprising the D4 domain through to the C6 domain. The distribution of variants did not differ significantly between domains, with each domain having between 70-79% of residues mutated (Table 1). Ultimately for the purpose of this study 9 single point mutations that had been previously reported but uncharacterised in detail were chosen for further investigation: Four were located in the D4 domain; Cys1950Tyr, Gly2044Asp, Cys2174Gly, Glu2233Gln. Three in the C2 domain; Cys2340Arg, Gly2343Val, Arg2379Cys and one each in the C4 and C6 domains; Ser2497Pro and Cys2693Tyr respectively (Table 2).[39-43] Two of the variants; Gly2044Asp and Cys2174Gly were categorised as type 3 VWD with the remaining variants predicted to be type 1. Both PolyPhen-2 and SIFT scores predicted all the mutations, with the exception of Ser2479Pro to be damaging or affect protein function (Table 2).

Mutations in the D4 and C-domains affect VWF expression

The selected mutations were generated in the expression vector pcDNA3.1-FL-VWF and transiently expressed in HEK293T cells and VWF levels in both media and lysate quantified by ELISA. Compared to wtVWF all the variants demonstrated significantly reduced secretion. In keeping with their type 3 VWD phenotype virtually no secretion was observed for the Gly2044Asp and Cys2174Gly variants (Figure 1A). No secretion was also observed for the Cys1950Y, Glu2233Gln, Cys2340Arg, Gly2343Val and Cys2693Tyr variants, indicating a detrimental effect on expression (Figure 1A). Significantly reduced levels were observed with the Arg2379Cys and Ser2497Pro variants (10 – 20% of normal). Interestingly, all the mutant proteins were present in the cell lysate at a similar level to wtVWF, with the exception of VWF-Glu2233Gln (Figure 1B).

Expression of more some VWD mutants cannot be rescued by co-expression of WT VWF

Since many of these mutations are likely to be heterozygous, transfections were repeated co-expressing wtVWF alongside the variant protein. Co-expression with wtVWF increased VWF secretion to varying extents, however this rarely exceeded 50% of normal (Figure 2A). In order to investigate if the secreted protein comprised a mixture of wild type and variant protein, co-transfections were

Journal Pre-proof

repeated where the full length expression vector containing the desired mutation was transfected alongside a VWF-ΔA1 construct that lacks the A1 domain. As shown in figure 2B, when run on reducing SDS-PAGE gel the ΔA1 monomers migrate faster than full length monomers allowing a ratio of the two to be determined. When transfected alongside full length VWF, the ratio of wtVWF/ΔA1 is approximately 1:1. The Gly2044Asp, Gal2343Val, Ser2497Pro and Cys2693Tyr variants were secreted in an approximately 1:1 ratio with VWF- ΔA1 showing that these could be incorporated into released VWF (Figure 2B&C). However for the Cys1950Tyr, Cys2174Gly, Glu2233Gln, Cys2340Arg and Arg2379Cys variants there was virtually no mutant monomer secreted, with the ΔA1-band the predominant species visible, indicating that these mutations result in VWF molecules that cannot be incorporated into secreted multimers and the "rescued" VWF expression in our HEK293T cells expression system represents mostly expression of wild type VWF (Figure 2B&C). Together these data demonstrate that mutations in the D4 and C-domains can have a dramatic impact on VWF expression and secretion.

D4 and C-domain variants give rise to abnormal intra-cellular multimers

To further characterise the C-terminal variants multimer gel analysis was performed on cell lysates from cells transfected with the variants in the homozygous state. In keeping with previously published reports the cell lysates contained mainly lower order VWF species rather than a full spectrum of multimers [44] (Figure 3). Except for the Arg2379Cys variant, all the mutant proteins, like wtVWF, showed the clear presence of dimers, with 1 or 2 feint bands of higher order multimers visible, suggesting that at least some protein was trafficked to the Golgi body for multimerization to occur (Figure 3). Strikingly however, a number of differences were observed between the variant proteins compared to wtVWF. The Cys1950Tyr, Cys2174Gly, Glu223Gln, Gly2343Val, Ser2497Pro and Cys2693Tyr proteins all presented bands that migrated faster than the equivalent wtVWF band, this was particularly apparent for the dimer band. Moreover, although not as distinct, the Gly2044Asp and Cys2340Arg variants also exhibited faster migrating bands. These bands shifts may indicate either aberrant protein folding, disulphide bond formation or differences in glycosylation. The Arg2379Cys variant showed a virtual absence of dimers with mostly monomers present in the lysate, indicating a failure to properly form dimers.

VWD mutations fail to form pseudo Weibel-Palade bodies

Since in the homozygous state all the investigated mutations either had abolished or significantly reduced secretion with abnormal multimers in the cell lysate it was next investigated if the mutants could form pseudo-WPBs following expression in HEK293 cells. HEK293 cells were used for

these experiments since the 293T counterparts fail to form pseudo-WPBs. Following transfection, cells were fixed and stained with antibodies against VWF, and the endoplasmic reticulum (ER) marker Protein Disulphide Isomerase (PDI). HEK293 cells expressing wtVWF showed a staining pattern of VWF co-localisation in the ER and in keeping with previous data, HEK293 cells transfected with wtVWF could form distinct structures that stained positive for VWF, consistent with being pseudo-WPBs (Figure 4). Interestingly, not every cell that expressed VWF formed pseudo-WPBs with ~30% of cells presenting structures deemed to be pseudo-WPBs. Strikingly, none of the mutants were able to form discernible numbers of pseudo-WPBs (Figure 4), with the staining being limited to VWF localised within the ER. Another observation was that in both wtVWF and mutant expressing cells dense, strongly staining structures were observed that demonstrated co-localisation of VWF to the ER, indicating potential areas of the ER swollen with VWF (Figure 4 – see white arrows). While these were present with wtVWF, they were more frequently observed with the mutants.

Arg2379Cys in the homozygous state is a novel type 2A mutation

Since the Arg2379Cys and Ser2947Pro mutants could be secreted to some degree we over-expressed these mutants and concentrated the medium to allow multimeric and functional analysis of the secreted VWF. The Ser2497Pro mutant had a normal multimeric distribution compared to wtVWF, however consistent with the observations made with the cell lysate samples, the Arg2379Cys mutation was only present in the secreted media as mostly monomers and a faster migrating band, with a very faint dimer band visible (Figure 5A). Previously the Arg2379Cys mutant was suggested to be a type 1 mutation.[42] However, the absence of secreted multimers suggests that in the homozygous state, Arg2379Cys is a type 2A, group I mutation. To investigate the impact of the Arg2379Cys mutation further, HEK293T cells were transfected with a VWF construct encoding the A2-CK domains and media and lysate samples were harvested at different time points post-transfection. As expected, wtVWF-A2CK presented both monomers and dimers in the lysate that were finally secreted as dimers. In comparison, Arg2379Cys-A2-CK failed to form appreciable dimers in the cell and only monomers could be secreted, albeit at a lesser and slower extent than wt-A2CK. It was also observed that the Arg2379Cys-A2-CK bands in the cell lysate migrated further than the wt-A2CK bands indicating either an altered structure or abnormal glycosylation (Figure 5B). Finally, to investigate the functionality of the Arg2379Cys or Ser2497Pro mutants in response to shear, flow assays were performed perfusing plasma-free blood supplemented with either wtVWF, or mutant VWF and perfused over type III collagen at $1500s^{-1}$. As expected, no platelet capture was observed with the Arg2379Cys mutant since it lacked functional multimers (Figure 5C). Ser2497Pro demonstrated a normal platelet capture profile similar to wtVWF indicating that this mutation does not cause a

Journal Pre-proof

functional defect (Figure 5C). Together this data shows that the Arg2379Cys mutation in its homozygous state causes a type 2A phenotype by preventing dimer formation in the ER while the Ser2497Pro mutant is unlikely to be functionally pathogenic and may be characterised as a type 1 mutation.

Structural impact of the VWD mutations

To understand the impact of the mutations further we mapped the mutations on to structural models of the D4 assembly and the C-domains. Currently only NMR structures have been obtained for the C4 and C6 domains thus a model of the D4 and C-domains was generated. Based on our model, Cys1950 is located in the VWD4 part of the assembly and forms a buried disulphide bond with Cys2085 (Figure 6A). Gly2044 is also buried occurs at the interface of the VWD4 and TIL4 sub-domains (Figure 6A). Mutation of both these residues is therefore likely to cause structural defects. Cys2174 is in the C8-4 domain and our model predicts a disulphide bond with C2199 in the TIL-4 domain, loss of this disulphide is likely to weaken the C8-4 – TIL-4 interface (Figure 6A). Finally in the D4 assembly, Glu2233 forms a potential salt bridge with Arg2194 which would be lost with the mutation (Figure 6A). In the C2 domain Cys2340 forms a disulphide bond with Cys2360, the loss of the bond is likely to destabilise the structure (Figure B). The role of Gly2343 is less clear, it occurs close to the junction between the 2 subdomains of the C3 domain and could therefore affect conformation (Figure 6B). Arg2379 lies in close proximity to 3 disulphide bonds and the introduction of a new cysteine residue may therefore result in aberrant cysteine bonds forming (Figure 6B). Ser2497 occurs on the junction between the C3 and C4 domain, but it is not clear how mutation of this will impact the structure (Figure 6C). Finally, Cys2693 was mapped onto the NMR structure of the C6 domain and forms a disulphide with Cys2716 and again loss of this bond is likely to destabilise the domain (Figure 6D).

Journal Pre-proof

Discussion

In this study we have examined nine mutations identified in VWD patients that are predicted to be causative mutations located in the D4 and C-domains of VWF. With the exception of Arg2379Cys and Ser2497Pro, all the variants failed to be secreted from HEK293T cell indicting that in the homozygous state these mutations are highly detrimental to VWF expression. Two of the variants; Gly2044Asp and Cys2174Gly had been previously reported in patients with type 3 VWD.[40, 45] In the case of the latter, the index case was homozygous for the Cys2714Gly mutation, while the index case with the Gly2044Asp mutation was compound heterozygous with two other mutations Gly19Arg and Cys2491Arg.[40] Previously we have shown that Cys2491Ala cannot be secreted from HEK293T cells and thus a Cys2491Arg mutation would likely have the same effect.[34] And previous recombinant expression of the Gly19Arg did not demonstrated any effect on VWF expression[46]. The Gly2044Asp variant alone was catastrophic enough to ablate secretion and may therefore be considered a type 3 causative mutation in the homozygous state. Since the majority of VWD patients are heterozygous we attempted to mimic this by co-transfecting the variant VWF alongside wild type. While this rescued expression to varying degrees it was unable to restore expression to that of wtVWF alone. However, although expression can be rescued with co-transfection with wtVWF, this does not necessarily infer that the mutant VWF monomers are forming part of the secreted monomer. Co-transfections with the VWF-ΔA1 construct allowed us to distinguish mutant and "normal" monomers in the secreted protein. Interestingly despite ablating secretion, Gly2044Asp was secreted in an ~1:1 ratio with VWF-ΔA1, thus the mutant monomers could be at least to some extent incorporated into the secreted protein. Therefore in the reported type 3 case with Gly2044Asp the compound heterozygous status with Cys2491Arg results in type 3 VWD. Similarly, the Glu2343Val, Ser2497Pro and Cys2693Tyr variants could all be secreted to some extent with VWF-ΔA1. For the remaining variants only the VWF-ΔA1 band was visible indicating that the variant monomer was unable to be rescued. It is not clear why some mutants can be rescued, and others cannot, but the structural change caused by the mutations is likely to be a key factor. It is generally accepted that all of the cysteine residues in VWF are engaged in disulphide bond formation, except for disulphides implicated in multimer formation, this occurs within the ER and is critical for proper secretion.[34, 47] Therefore, mutations affecting cysteine residues are likely to have a serious structural impact and our structural models suggest the loss of cysteine residues is extremely likely to result in domain destabilisation and mis-folding and will prevent exit from the ER, even when a dimer is formed with an unaffected wild-type monomer. Interestingly, the Cys2693Tyr mutant was able to demonstrate rescue, indicating that the loss of this cysteine could be tolerated to some degree, possibly because this cysteine occurs towards the end of the primary amino sequence and may partake in one of the final disulphide bonds to be formed. For

Journal Pre-proof

the remaining mutants our structural analysis demonstrates that loss of certain residues can potentially alter sub-domain interactions, especially in the D4 assembly. It should however be noted that with the exception of the C6 domain, these are only putative models and need to be interpreted with a degree of caution.

Multimer analysis of the cell lysates failed to reveal a full spectrum of multimers for wtVWF or the mutants; however, this is in keeping with previous observations that follow the expression of VWF in heterologous cell systems.[44, 48, 49] The reason for this has not been resolved. HEK293T cells secrete a full range of VWF multimers and while the proportion of smaller order multimeric species is generally higher than that of normal plasma, recombinant expressed VWF tends to also exhibit larger multimers than those found in plasma, presumably due to the lack of ADAMTS13. The absence of a full multimer range in the cell lysate could represent rapid passage from the ER to the secretion pathway and indeed in this study, positive co-staining for VWF in the Golgi body was not observed (data not shown). Apart from Gly2044Asp and Arg2379Cys, all the mutants and wtVWF show the presence of dimers, and one or two higher order bands and a clear smear pattern. Nonetheless, there were some notable differences between wtVWF and the mutants. Most striking for all the mutants the dimer band migrated visibly further, indicating either defective glycosylation or altered structure. N-linked glycosylation occurs co-translationally with the addition of the pre-cursor glycan structure to the nascent peptide and after several trimming steps in the ER, glycosyltransferases add sugars to the glycan chains within the Golgi.[50] While altered glycosylation cannot be ruled out, it is unlikely since dimers and some higher-order species are being formed. The altered migration may therefore represent abnormal folding of the protein and in the case of the cysteine mutations could be due to aberrant disulphide bonds being formed.

Immunofluorescent analysis of transfected cells further confirmed the synthesis defects, with none of the mutations forming appreciable pseudo-WPBs. It is noteworthy however that not all cells transfected with wtVWF formed WPBs, we observed ~30% of cells forming WPB like structures. Michaux *et al* previously reported up to ~60% of transfected HEK293 forming WPBs, however other studies using the HEK293 cell model have not reported the proportion of cells expressing wtVWF. Another key observation was that the majority of the VWF staining co-localised with the ER. Although not shown, no co-localisation was seen with the Golgi, although this may reflect limitations in the experimental method. Interestingly, several cells demonstrated dense, punctate areas of VWF staining that could be mistaken for WPBs, however these co-localised with the ER marker. While these were more prominent in mutant-expressing cells, some wtVWF-expressing cells also formed similar structures. While further work is needed to precisely define the nature of these structures, they likely

represent an ER that is overloaded with VWF. Interestingly, the stained structures are similar to organised smooth ER (OSER) that can be formed when the ER is transformed from a network of branching tubules into stacked membrane arrays.[51] This process can occur when there is overexpression of proteins. Therefore, the overexpression of VWF in the HEK293 cell system and the enhanced ER retention observed with the variants may result in OSER formation.

Since for the Arg2379Cys and Ser2497Pro mutants some secretion was observed, these were overexpressed to obtain protein for functional analysis. Secreted Ser2497Pro formed normal multimers and behaved similar to wtVWF under flow conditions at $1500s^{-1}$ indicating that no functional defects were caused by this mutation. Strikingly, the Arg2379Cys mutant failed to form multimers with only the appearance of monomers and few dimers and a band that migrated faster than the monomer. As expected, Arg2379Cys could not capture platelets under flow, consistent with the lack of multimers. When expressed as dimeric A2CK, the Arg2379Cys mutant failed to form dimers in the cell lysate and was secreted as monomers, confirming the defective dimerisation. It was also observed that the Arg2379Cys monomers migrated further than the wtA2CK monomers. The introduction of a new cysteine residue is likely to have a significant impact on the protein structure. Based on our structural model of the C domains, several cysteine residues reside in close proximity to Arg2379: Cys2375, Cys2396 and Cys2398. It is probable that the new cysteine at position 2379 may potentially form an aberrant disulphide with any of these and disrupt proper protein folding. Together this data indicates that in the homozygous state, Arg2379Cys would be a type 2A mutation that disrupts normal multimer formation. Although this variant has only yet been identified as heterozygous and is not associated with a severe bleeding phenotype, it highlights that mutations in VWF can cause different types of disease depending on their hetero- or homozygosity. Similarly, for the cysteine mutations characterised in this study the heterozygous state is likely to lead to type 1 VWD with a reduction in levels of essentially normal VWF, while in a homozygous state or compound heterozygous state with other mutations can lead to abolished expression. This potentially should be considered when genetically counselling patients with VWD.

Finally, although VWF clearance has not been investigated in this study, it may be postulated that heterozygous multimers may be subject to faster clearance and warrants further investigation. In summary, this data sheds light on the phenotype of nine previously described but uncharacterised mutations and highlights how mutations can behave differently depending on being homo or heterozygous.

Journal Pre-proof

Journal Pre-proof

Author contributions: G.M designed the study, performed experiments, analysed results, and wrote the manuscript. S.EM performed experiments, analysed results, and wrote the manuscript. A.C. performed experiments and wrote the manuscript. T.D.N Analysed results, and wrote the manuscript. T.A.J.M designed the study, performed experiments, analysed results, and wrote the manuscript.

Declaration of competing Interests: There are no competing interests to disclose.

Funding information: This work was funded by a British Heart Foundation PhD fellowship (FS/20/9/34989) awarded to G.M and T.A.J.M. We are grateful for support from the Imperial College BRC

Journal Pre-proof

Journal Pre-proof

Table 1. Distribution of VWF mutations in the D4 assembly and C-domains

Domain	No. of residues	No. of mutations	% of amino acids mutated
D4 assembly	382	276	72.3
C1	79	56	70.1
C2	69	50	72.5
Linker	26	20	76.9
C3	68	48	70.6
C4	81	64	79
C5	69	53	76.8
C6	76	56	73.7
	Total 850	Total 623	Average 73.3%

Journal Pre-proof

Table 2. Characteristics and *in-silico* prediction of nine VWD causative mutations

DNA change	Amino acid change	Domain	Clinical data				Genotype	Predicted VWD type	PolyPhen-2		SIFT		Ref
			VWF: Ag	VWF: Rcof	VWF: CB	Multimers			Confidence score	Prediction	Score	Prediction	
c.5849G>A	Cys1950Tyr	D4 (VWD4)	23	14	-	-	Het	Type 1	1.00	PD	0.00	APF	39
c.6131G>A	Gly2044Asp	D4 (VWD4)	2	5	-	absent	C/Het	Type 3	1.00	PD	0.00	APF	40
c.6520T>G	Cys2174Gly	D4 (C8-4)	1	-	-	-	Hom	Type 3	1.00	PD	0.00	APF	41
c.6697G>C	Glu2233Gln	D4 (TLI-4)	25	18	-	-	Het	Type 1	1.00	PD	0.00	APF*	-
c.7018T>C	Cys2340Arg	C2	27	25	-	-	Het	Type 1	1.00	PD	0.00	APF	42
c.7028G>T	Gly2343Val	C2	45	41	-	-	Het	Type 1	1.00	PD	0.00	APF*	42
c.7135C>T	Arg2379Cys	C2	29	35	-	-	Het	Type 1	0.00	PD	0.04	APF*	42
c.7489TT>C	Ser2497Pro	C4	27	25	-	-	Het	Type 1	1.00	Benign	0.28	Tolerated	42
c.8078G>A	Cys2693Tyr	C6	46	64	42	normal	Het	Type 1	1.00	PD	0.00	APF*	43

Het = hetrozygous, C/Het =compound heterozygous, Hom = homozygous, PD = probably damaging, APF = affect protein function, APF* = affect protein function with low degree of certainty

Journal Pre-proof

References

1 Sadler JE. Biochemistry and genetics of von Willebrand factor. *Annu Rev Biochem*. 1998; **67**: 395-424. 10.1146/annurev.biochem.67.1.395.

2 Federici AB. The factor VIII/von Willebrand factor complex: basic and clinical issues. *Haematologica*. 2003; **88**: EREP02.

3 Jaffe EA, Hoyer LW, Nachman RL. Synthesis of von Willebrand factor by cultured human endothelial cells. *Proc Natl Acad Sci U S A*. 1974; **71**: 1906-9. 10.1073/pnas.71.5.1906.

4 Sporn LA, Chavin SI, Marder VJ, Wagner DD. Biosynthesis of von Willebrand protein by human megakaryocytes. *J Clin Invest*. 1985; **76**: 1102-6. 10.1172/JCI112064.

5 Wagner DD. Cell biology of von Willebrand factor. *Annu Rev Cell Biol*. 1990; **6**: 217-46. 10.1146/annurev.cb.06.110190.001245.

6 Zhou YF, Eng ET, Zhu J, Lu C, Walz T, Springer TA. Sequence and structure relationships within von Willebrand factor. *Blood*. 2012; **120**: 449-58. 10.1182/blood-2012-01-405134.

7 Wise RJ, Pittman DD, Handin RI, Kaufman RJ, Orkin SH. The propeptide of von Willebrand factor independently mediates the assembly of von Willebrand multimers. *Cell*. 1988; **52**: 229-36. 10.1016/0092-8674(88)90511-9.

8 Voorberg J, Fontijn R, Calafat J, Janssen H, van Mourik JA, Pannekoek H. Assembly and routing of von Willebrand factor variants: the requirements for disulfide-linked dimerization reside within the carboxy-terminal 151 amino acids. *J Cell Biol*. 1991; **113**: 195-205. 10.1083/jcb.113.1.195.

9 Purvis AR, Gross J, Dang LT, Huang RH, Kapadia M, Townsend RR, Sadler JE. Two Cys residues essential for von Willebrand factor multimer assembly in the Golgi. *Proc Natl Acad Sci U S A*. 2007; **104**: 15647-52. 10.1073/pnas.0705175104.

10 Przeradzka MA, van Galen J, Ebberink E, Hoogendijk AJ, van der Zwaan C, Mertens K, van den Biggelaar M, Meijer AB. D' domain region Arg782-Cys799 of von Willebrand factor contributes to factor VIII binding. *Haematologica*. 2020; **105**: 1695-703. 10.3324/haematol.2019.221994.

11 Shiltagh N, Kirkpatrick J, Cabrita LD, McKinnon TA, Thalassinos K, Tuddenham EG, Hansen DF. Solution structure of the major factor VIII binding region on von Willebrand factor. *Blood*. 2014; **123**: 4143-51. 10.1182/blood-2013-07-517086.

12 Flood VH, Gill JC, Christopherson PA, Bellissimo DB, Friedman KD, Haberichter SL, Lentz SR, Montgomery RR. Critical von Willebrand factor A1 domain residues influence type VI collagen binding. *J Thromb Haemost*. 2012; **10**: 1417-24. 10.1111/j.1538-7836.2012.04746.x.

13 Huizinga EG, Martijn van der Plas R, Kroon J, Sixma JJ, Gros P. Crystal structure of the A3 domain of human von Willebrand factor: implications for collagen binding. *Structure*. 1997; **5**: 1147-56. 10.1016/s0969-2126(97)00266-9.

14 Morales LD, Martin C, Cruz MA. The interaction of von Willebrand factor-A1 domain with collagen: mutation G1324S (type 2M von Willebrand disease) impairs the conformational change in A1 domain induced by collagen. *J Thromb Haemost*. 2006; **4**: 417-25. 10.1111/j.1538-7836.2006.01742.x.

15 Deng W, Wang Y, Druzak SA, Healey JF, Syed AK, Lollar P, Li R. A discontinuous autoinhibitory module masks the A1 domain of von Willebrand factor. *J Thromb Haemost*. 2017; **15**: 1867-77. 10.1111/jth.13775.

16 Zhang Q, Zhou YF, Zhang CZ, Zhang X, Lu C, Springer TA. Structural specializations of A2, a force-sensing domain in the ultralarge vascular protein von Willebrand factor. *Proc Natl Acad Sci U S A*. 2009; **106**: 9226-31. 10.1073/pnas.0903679106.

17 Zanardelli S, Chion AC, Groot E, Lenting PJ, McKinnon TA, Laffan MA, Tseng M, Lane DA. A novel binding site for ADAMTS13 constitutively exposed on the surface of globular VWF. *Blood*. 2009; **114**: 2819-28. 10.1182/blood-2009-05-224915.

18 Beacham DA, Wise RJ, Turci SM, Handin RI. Selective inactivation of the Arg-Gly-Asp-Ser (RGDS) binding site in von Willebrand factor by site-directed mutagenesis. *J Biol Chem*. 1992; **267**: 3409-15.

19 Seidizadeh O, Eikenboom JCJ, Denis CV, Flood VH, James P, Lenting PJ, Baronciani L, O'Donnell JS, Lillicrap D, Peyvandi F. von Willebrand disease. *Nat Rev Dis Primers*. 2024; **10**: 51. 10.1038/s41572-024-00536-8.
20 Lillicrap D. von Willebrand disease: advances in pathogenetic understanding, diagnosis, and therapy. *Blood*. 2013; **122**: 3735-40. 10.1182/blood-2013-06-498303.
21 Flood VH, Garcia J, Haberichter SL. The role of genetics in the pathogenesis and diagnosis of type 1 Von Willebrand disease. *Curr Opin Hematol*. 2019; **26**: 331-5. 10.1097/MOH.0000000000000524.
22 de Jong A, Eikenboom J. Von Willebrand disease mutation spectrum and associated mutation mechanisms. *Thromb Res*. 2017; **159**: 65-75. 10.1016/j.thromres.2017.09.025.
23 Riddell AF, Gomez K, Millar CM, Mellars G, Gill S, Brown SA, Sutherland M, Laffan MA, McKinnon TA. Characterization of W1745C and S1783A: 2 novel mutations causing defective collagen binding in the A3 domain of von Willebrand factor. *Blood*. 2009; **114**: 3489-96. 10.1182/blood-2008-10-184317.
24 McKinnon TA, Nowak AA, Cutler J, Riddell AF, Laffan MA, Millar CM. Characterisation of von Willebrand factor A1 domain mutants I1416N and I1416T: correlation of clinical phenotype with flow-based platelet adhesion. *J Thromb Haemost*. 2012; **10**: 1409-16. 10.1111/j.1538-7836.2012.04760.x.
25 Chegeni R, Vickars L, Favaloro EJ, Lillicrap D, Othman M. Functional analysis of three recombinant A1-VWF domain mutants in comparison to wild type and plasma-derived VWF facilitates subtyping in type 2 von Willebrand disease. *Thromb Res*. 2011; **127**: 161-6. 10.1016/j.thromres.2010.11.006.
26 Castaman G, Giacomelli SH, Jacobi P, Obser T, Budde U, Rodeghiero F, Haberichter SL, Schneppenheim R. Homozygous type 2N R854W von Willebrand factor is poorly secreted and causes a severe von Willebrand disease phenotype. *J Thromb Haemost*. 2010; **8**: 2011-6. 10.1111/j.1538-7836.2010.03971.x.
27 Englender T, Lattuada A, Mannucci PM, Sadler JE, Inbal A. Analysis of Arg834Gln and Val902Glu type 2A von Willebrand disease mutations: studies with recombinant von Willebrand factor and correlation with patient characteristics. *Blood*. 1996; **87**: 2788-94.
28 Ahmad F, Jan R, Kannan M, Obser T, Hassan MI, Oyen F, Budde U, Saxena R, Schneppenheim R. Characterisation of mutations and molecular studies of type 2 von Willebrand disease. *Thromb Haemost*. 2013; **109**: 39-46. 10.1160/TH12-07-0475.
29 Baronciani L, Federici AB, Beretta M, Cozzi G, Canciani MT, Mannucci PM. Expression studies on a novel type 2B variant of the von Willebrand factor gene (R1308L) characterized by defective collagen binding. *J Thromb Haemost*. 2005; **3**: 2689-94. 10.1111/j.1538-7836.2005.01638.x.
30 Solimando M, Baronciani L, La Marca S, Cozzi G, Asselta R, Canciani MT, Federici AB, Peyvandi F. Molecular characterization, recombinant protein expression, and mRNA analysis of type 3 von Willebrand disease: Studies of an Italian cohort of 10 patients. *Am J Hematol*. 2012; **87**: 870-4. 10.1002/ajh.23265.
31 Pagliari MT, Baronciani L, Cordiglieri C, Colpani P, Cozzi G, Siboni SM, Peyvandi F. The dominant p.Thr274Pro mutation in the von Willebrand factor propeptide causes the von Willebrand disease type 1 phenotype in two unrelated patients. *Haemophilia*. 2022; **28**: 292-300. 10.1111/hae.14494.
32 Dubois MD, Peyron I, Pierre-Louis ON, Pierre-Louis S, Rabout J, Boisseau P, de Jong A, Susen S, Goudemand J, Neviere R, Fuseau P, Christophe OD, Lenting PJ, Denis CV, Casari C. Identification of von Willebrand factor D4 domain mutations in patients of Afro-Caribbean descent: In vitro characterization. *Res Pract Thromb Haemost*. 2022; **6**: e12737. 10.1002/rth2.12737.
33 Chen S, Francioli LC, Goodrich JK, Collins RL, Kanai M, Wang Q, Alfoldi J, Watts NA, Vittal C, Gauthier LD, Poterba T, Wilson MW, Tarasova Y, Phu W, Grant R, Yohannes MT, Koenig Z, Farjoun Y, Banks E, Donnelly S, Gabriel S, Gupta N, Ferriera S, Tolonen C, Novod S, Bergelson L, Roazen D, Ruano-Rubio V, Covarrubias M, Llanwarne C, Petrillo N, Wade G, Jeandet T, Munshi R, Tibbetts K, Genome Aggregation Database C, O'Donnell-Luria A, Solomonson M, Seed C, Martin AR, Talkowski ME, Rehm

HL, Daly MJ, Tiao G, Neale BM, MacArthur DG, Karczewski KJ. A genomic mutational constraint map using variation in 76,156 human genomes. *Nature*. 2024; **625**: 92-100. 10.1038/s41586-023-06045-0.

34 Shapiro SE, Nowak AA, Wooding C, Birdsey G, Laffan MA, McKinnon TA. The von Willebrand factor predicted unpaired cysteines are essential for secretion. *J Thromb Haemost*. 2014; **12**: 246-54. 10.1111/jth.12466.

35 Casari C, Pinotti M, Lancellotti S, Adinolfi E, Casonato A, De Cristofaro R, Bernardi F. The dominant-negative von Willebrand factor gene deletion p.P1127_C1948delinsR: molecular mechanism and modulation. *Blood*. 2010; **116**: 5371-6. 10.1182/blood-2010-02-268920.

36 O'Donnell J, Boulton FE, Manning RA, Laffan MA. Amount of H antigen expressed on circulating von Willebrand factor is modified by ABO blood group genotype and is a major determinant of plasma von Willebrand factor antigen levels. *Arterioscler Thromb Vasc Biol*. 2002; **22**: 335-41. 10.1161/hq0202.103997.

37 Baillod P, Affolter B, Kurt GH, Pflugshaupt R. Multimeric analysis of von Willebrand factor by vertical sodium dodecyl sulphate agarose gel electrophoresis, vacuum blotting technology and sensitive visualization by alkaline phosphatase anti-alkaline phosphatase complex. *Thromb Res*. 1992; **66**: 745-55. 10.1016/0049-3848(92)90050-k.

38 Webb B, Sali A. Comparative Protein Structure Modeling Using MODELLER. *Curr Protoc Protein Sci*. 2016; **86**: 2 9 1-2 9 37. 10.1002/cpps.20.

39 Downes K, Megy K, Duarte D, Vries M, Gebhart J, Hofer S, Shamardina O, Deevi SVV, Stephens J, Mapeta R, Tuna S, Al Hasso N, Besser MW, Cooper N, Daugherty L, Gleadall N, Greene D, Haimel M, Martin H, Papadia S, Revel-Vilk S, Sivapalaratnam S, Symington E, Thomas W, Thys C, Tolios A, Penkett CJ, BioResource N, Ouwehand WH, Abbs S, Laffan MA, Turro E, Simeoni I, Mumford AD, Henskens YMC, Pabinger I, Gomez K, Freson K. Diagnostic high-throughput sequencing of 2396 patients with bleeding, thrombotic, and platelet disorders. *Blood*. 2019; **134**: 2082-91. 10.1182/blood.2018891192.

40 Ahmad F, Budde U, Jan R, Oyen F, Kannan M, Saxena R, Schneppenheim R. Phenotypic and molecular characterisation of type 3 von Willebrand disease in a cohort of Indian patients. *Thromb Haemost*. 2013; **109**: 652-60. 10.1160/TH12-10-0737.

41 Baronciani L, Cozzi G, Canciani MT, Peyvandi F, Srivastava A, Federici AB, Mannucci PM. Molecular defects in type 3 von Willebrand disease: updated results from 40 multiethnic patients. *Blood Cells Mol Dis*. 2003; **30**: 264-70. 10.1016/s1079-9796(03)00033-0.

42 James PD, Notley C, Hegadorn C, Leggo J, Tuttle A, Tinlin S, Brown C, Andrews C, Labelle A, Chirinian Y, O'Brien L, Othman M, Rivard G, Rapson D, Hough C, Lillicrap D. The mutational spectrum of type 1 von Willebrand disease: Results from a Canadian cohort study. *Blood*. 2007; **109**: 145-54. 10.1182/blood-2006-05-021105.

43 Goodeve A, Eikenboom J, Castaman G, Rodeghiero F, Federici AB, Batlle J, Meyer D, Mazurier C, Goudemand J, Schneppenheim R, Budde U, Ingerslev J, Habart D, Vorlova Z, Holmberg L, Lethagen S, Pasi J, Hill F, Hashemi Soteh M, Baronciani L, Hallden C, Guilliatt A, Lester W, Peake I. Phenotype and genotype of a cohort of families historically diagnosed with type 1 von Willebrand disease in the European study, Molecular and Clinical Markers for the Diagnosis and Management of Type 1 von Willebrand Disease (MCMDM-1VWD). *Blood*. 2007; **109**: 112-21. 10.1182/blood-2006-05-020784.

44 Michaux G, Hewlett LJ, Messenger SL, Goodeve AC, Peake IR, Daly ME, Cutler DF. Analysis of intracellular storage and regulated secretion of 3 von Willebrand disease-causing variants of von Willebrand factor. *Blood*. 2003; **102**: 2452-8. 10.1182/blood-2003-02-0599.

45 Baronciani L, Cozzi G, Canciani MT, Peyvandi F, Srivastava A, Federici AB, Mannucci PM. Molecular characterization of a multiethnic group of 21 patients with type 3 von Willebrand disease. *Thromb Haemost*. 2000; **84**: 536-40.

46 Eikenboom J, Hilbert L, Ribba AS, Hommais A, Habart D, Messenger S, Al-Buhairan A, Guilliatt A, Lester W, Mazurier C, Meyer D, Fressinaud E, Budde U, Will K, Schneppenheim R, Obser T, Marggraf O, Eckert E, Castaman G, Rodeghiero F, Federici AB, Batlle J, Goudemand J, Ingerslev J, Lethagen S, Hill F, Peake I, Goodeve A. Expression of 14 von Willebrand factor mutations identified in patients with

type 1 von Willebrand disease from the MCMDM-1VWD study. *J Thromb Haemost*. 2009; **7**: 1304-12. 10.1111/j.1538-7836.2009.03486.x.

47 Wagner DD, Marder VJ. Biosynthesis of von Willebrand protein by human endothelial cells: processing steps and their intracellular localization. *J Cell Biol*. 1984; **99**: 2123-30. 10.1083/jcb.99.6.2123.

48 Lyons SE, Bruck ME, Bowie EJ, Ginsburg D. Impaired intracellular transport produced by a subset of type IIA von Willebrand disease mutations. *J Biol Chem*. 1992; **267**: 4424-30.

49 Mayadas TN, Wagner DD. Vicinal cysteines in the prosequence play a role in von Willebrand factor multimer assembly. *Proc Natl Acad Sci U S A*. 1992; **89**: 3531-5. 10.1073/pnas.89.8.3531.

50 Kornfeld R, Kornfeld S. Assembly of asparagine-linked oligosaccharides. *Annu Rev Biochem*. 1985; **54**: 631-64. 10.1146/annurev.bi.54.070185.003215.

51 Snapp EL, Hegde RS, Francolini M, Lombardo F, Colombo S, Pedrazzini E, Borgese N, Lippincott-Schwartz J. Formation of stacked ER cisternae by low affinity protein interactions. *J Cell Biol*. 2003; **163**: 257-69. 10.1083/jcb.200306020.

Journal Pre-proof

Figure legends

Figure 1. Homozygous expression of recombinant VWF mutants. HEK293T cells were transfected with expression vectors for the D4 and C-domain mutants. Conditioned media and lysates were harvested 72 hours post-transfection, and the concentration of VWF was quantified using ELISA. Results were calculated relative to wtVWF expression as a percentage (%). (A) VWF levels in the media was virtually abolished for all mutants except for Arg2379Cys, Ser2497Pro and Cys2693Tyr. (B) VWF levels in cell lysates demonstrated comparable levels to wtVWF with the exception of Glu2233Gln which demonstrated a significant decrease in VWF:Ag levels. (Error bars represent the mean SD of 3 biological repeats performed in duplicate. **** p=<0.0001).

Figure 2. Heterozygous expression of recombinant VWF mutants. (A) HEK293T cells were transfected with expression vectors for wtVWF and the D4 or C-domain mutants. Conditioned media was harvested 72 hours post-transfection, and the concentration of VWF was quantified using ELISA. Results were calculated relative to wtVWF expression as a percentage (%). All mutants demonstrated rescued expression but were significantly reduced compared to wtVWF. (B) HEK293T cells were co-transfected with expression vectors for mutant VWF alongside VWF-ΔA1. 72 hours post-transfection, conditioned media was collected and analysed by SDS-PAGE and VWF was detected by western blot with anti-human VWF HRP-conjugated antibody. (C) The ratio between mutant and non-mutant monomer co-transfections were quantified using Image J. Mutants Gly2044Asp, Glu2343Val, Ser2497Pro and Cys2693Tyr demonstrated rescued expression when co-transfected with VWF-ΔA1 while Cys1950Tyr and Cys2340Arg failed to express mutant VWF. Cys2174Gly, Glu2233Gln, and Cys2340Arg mainly expressed VWF-ΔA1 with minimal mutant protein expression. (Error bars represent the mean SD of 3 biological repeats performed in duplicate. *** p=<0.001 **** p=<0.0001)

Figure 3. Multimeric Composition of the VWD Mutant Lysates. The multimeric pattern of the variants in the cell lysate was assessed by 1.2% non-reducing agarose gel electrophoresis. Samples were diluted to 5µg/mL of VWF and 10µl loaded onto the gel reference plasma as control. The gel was subsequently visualised by western blotting with polyclonal anti-VWF-HRP antibody. All mutants demonstrated dimers and some low molecular weight multimers except Arg2379Cys which mainly presented monomers. Dimer bands for Cys1950Tyr, Cys2174Gly, Glu2233Gln, Gly2343Val, Ser2497Pro and Cys2693Tyr migrated further compared to wtVWF and reference plasma. (Representative example of multimer gel performed in duplicate).

Figure 4. Intracellular analysis of VWD mutants. (A) HEK293 cells were transfected with expression vectors for wtVWF or the VWD mutants and subsequently fixed with 4% PFA and permeabilised with

0.1% Triton X. Cells were stained with anti-VWF FITC (green) and antibodies against PDI (red) followed by secondary Alexafluor-555 conjugated antibody. Nuclei were stained with DAPI (blue). Cells were visualised at x63 magnification under a Zeiss LSM800 confocal microscope All mutants demonstrated large areas of co-localisation that were consistent with VWF present in the ER. pseudo-WPBs were observed only with wtVWF (indicated by white arrow on wtVWF image). Some large punctate structures were also observed that stained positive for VWF and the ER (indicated by white arrows on the Gly2044Asp and Arg2379Cys images).

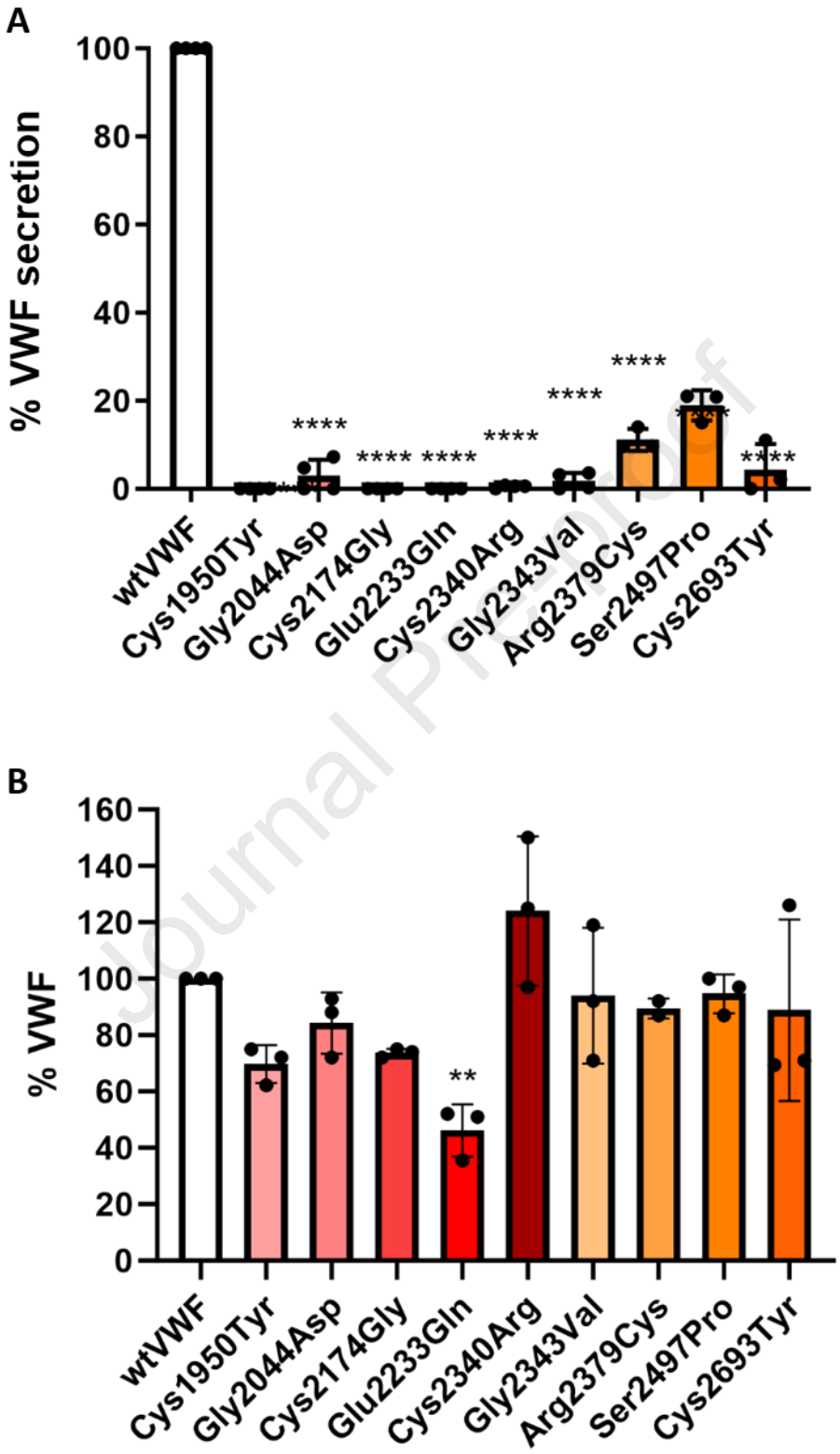
Figure 5. Analysis of Arg2379cys and Ser2497Pro mutants. (A) The multimeric composition of the Arg2379Cys and Ser2497Pro mutants was analysed by non-reducing agarose gel electrophoresis. Samples were prepared using 5 µg/mL of protein, alongside wtVWF and reference plasma as controls. The gel was subsequently visualised by western blotting with polyclonal anti-VWF-HRP antibody. Arg2379Cys demonstrated predominantly monomeric VWF with a feint dimer band. Ser2497Pro presented a normal multimeric profile similar to wtVWF and reference plasma. (B) HEK293T cells were transfected with expression vectors for either wtA2CK or A2CK containing the Arg2379Cys mutation. Cell lysate and media samples were harvested at different time points post-transfection and analysed by non-reducing SDS-PAGE. As a control reduced wild type A2CK protein (*) was run alongside the media and lysate samples. wtA2CK presented as both monomers and dimers in the lysate but was secreted in the dimeric form. Arg2379Cys-A2CK was only present as faster migrating monomers in the cell lysate and could only be secreted in small amounts in the monomeric form. (C) Ibidi® µ-Slides $V^{0.1}$ flow chamber slides were coated overnight with human type III collagen. Plasma-free blood was prepared by washing red blood cells and platelets followed by labelling of platelets with $DiOC_6$ for visualisation. The plasma-free blood was then supplemented with 2.5 µg/ml of VWF and perfused over the collagen-coated channels at a shear rate of $1500s^{-1}$. Ser2497Pro displayed a normal platelet capture profile compared to wtVWF while Arg2379Cys failed to support platelet capture. A representative image from three biological replicates (n=3) is depicted.

Figure 6. Structural analysis of VWD mutants. A model of the D4 assembly and the C-domains was generated using Modeller based on the porcine Alphafold template as described in materials and methods. (A) Location of mutants in the D4 assembly. The D4 assembly comprised of D4N (yellow), VWD4 (magenta), C8-4 (green) and TIL-4 (cyan) is shown. Cys1950 shown in yellow occurs in the VWD4 sub-domain and forms a buried disulphide bridge with Cys2085 shown in lime green. Gly2044 (shown in blue) is located at the VWD4-TIL4 interface. Cys2174 shown in yellow is located on an alpha-helix in the C8-4 subdomain, and Glu2233 shown in purple occurs on the TIL-4 domain. (Aii) Glu2233 forms a potential salt bridge with Arg2194 which is shown red and is located in the TIL-4 sub-domain. (B) A

model of the VWF C2 domain showing the C2 domain (yellow) and the linker region (silver). Cys2340 shown in red forms a disulphide bond with Cys2360. Gly2343 shown in blue is located at the junction of the two C2 sub-domains. Arg2379 shown in red is located in close proximity to three putative disulphide bonds. (C) A model of the VWF C3C4 domains showing the C3 domain (green) and C4 domain (cyan). Ser2497 is located at the junction between the two domains. (D) NMR structure of the C6 domain showing Cys2693 that forms a disulphide bond with Cys2716.

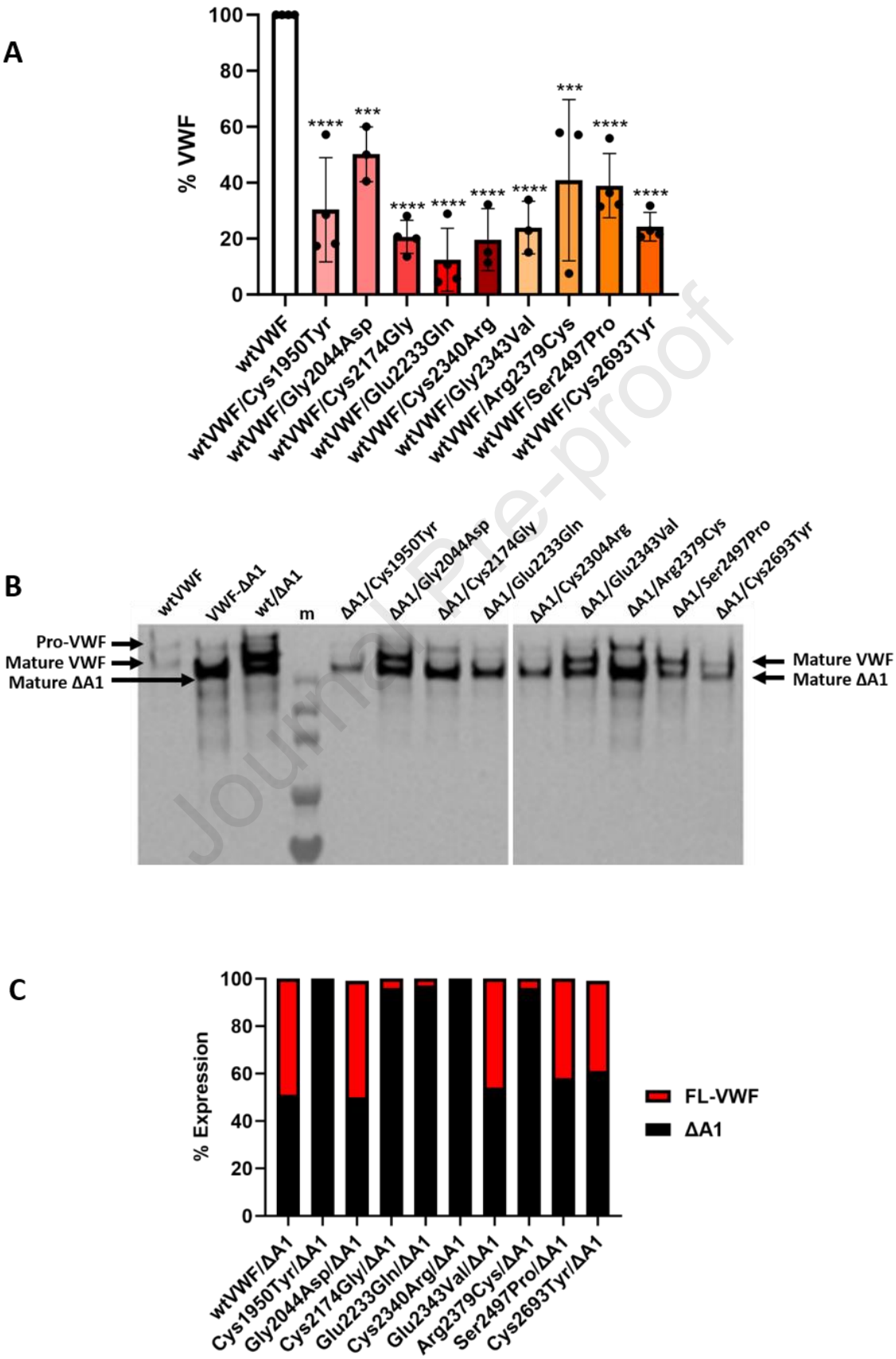
Journal Pre-proof

Figure 1



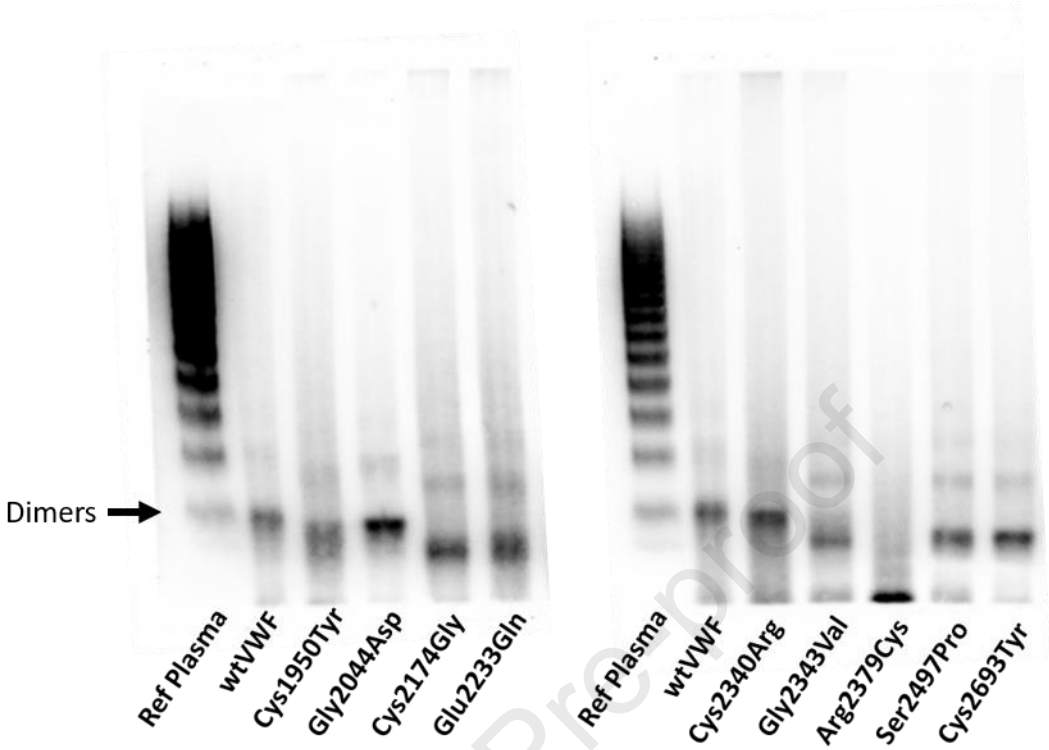
Journal Pre-proof

Figure 2



Journal Pre-proof

Figure 3



Journal Pre-proof

Figure 4

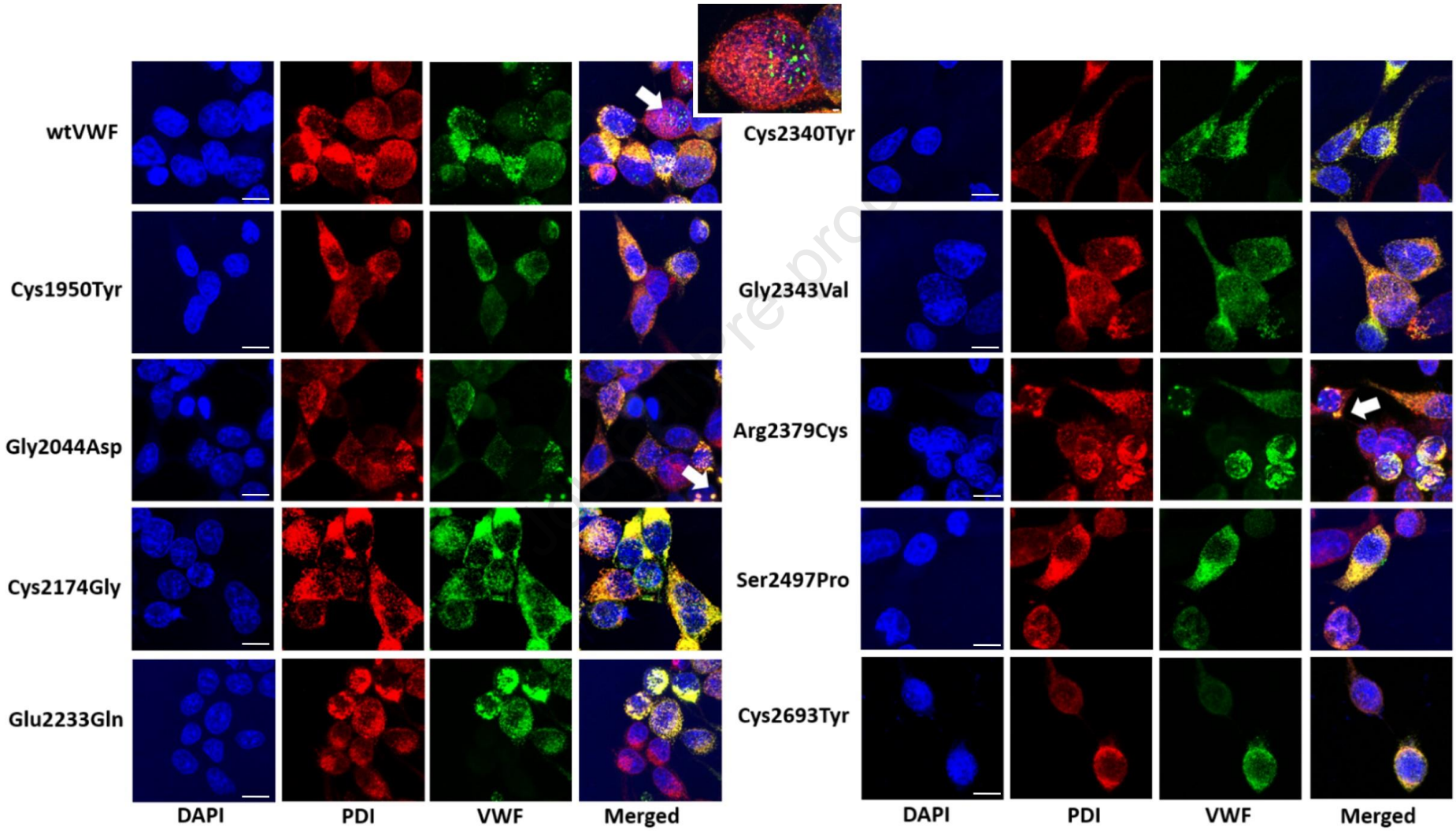
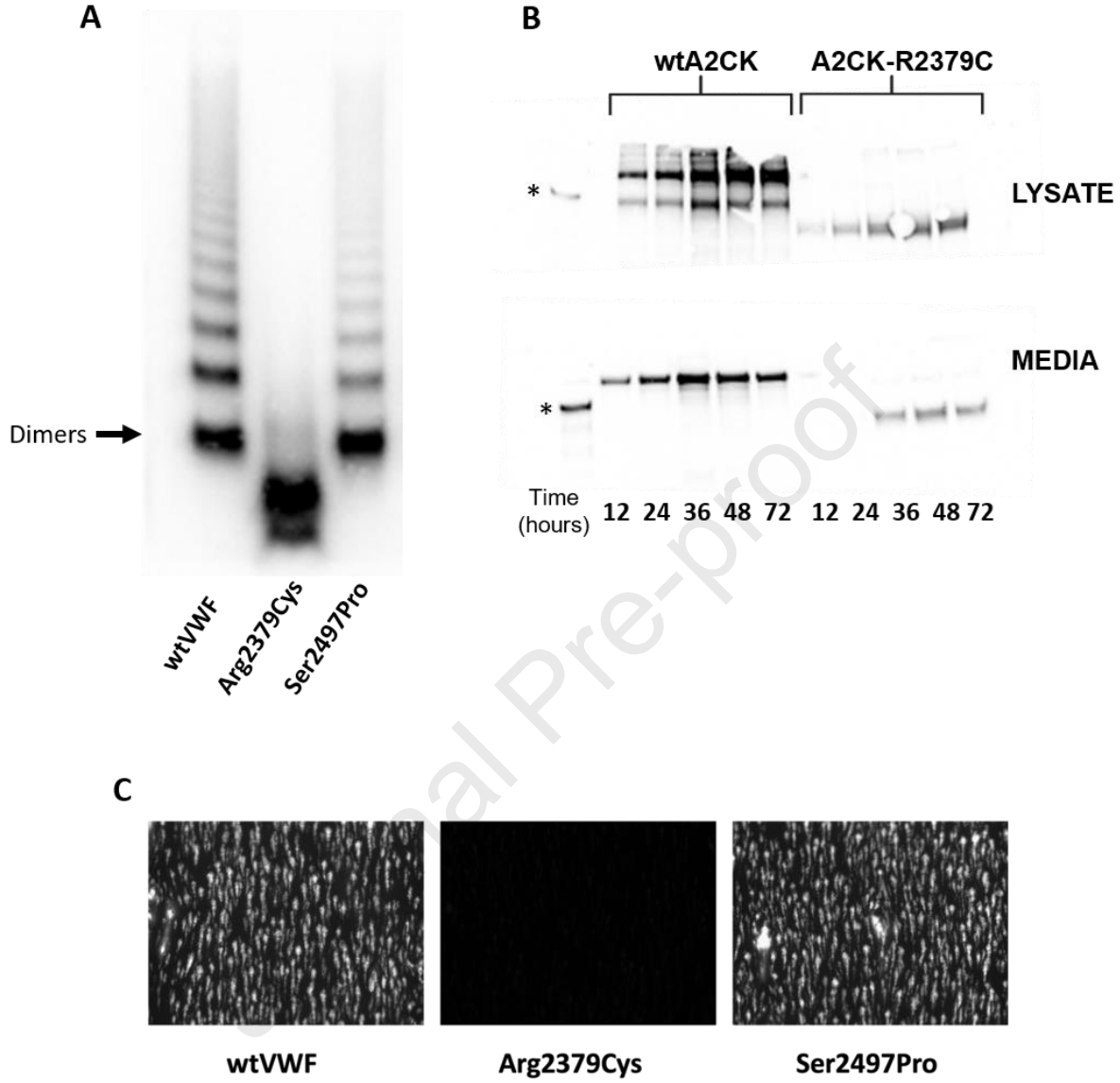
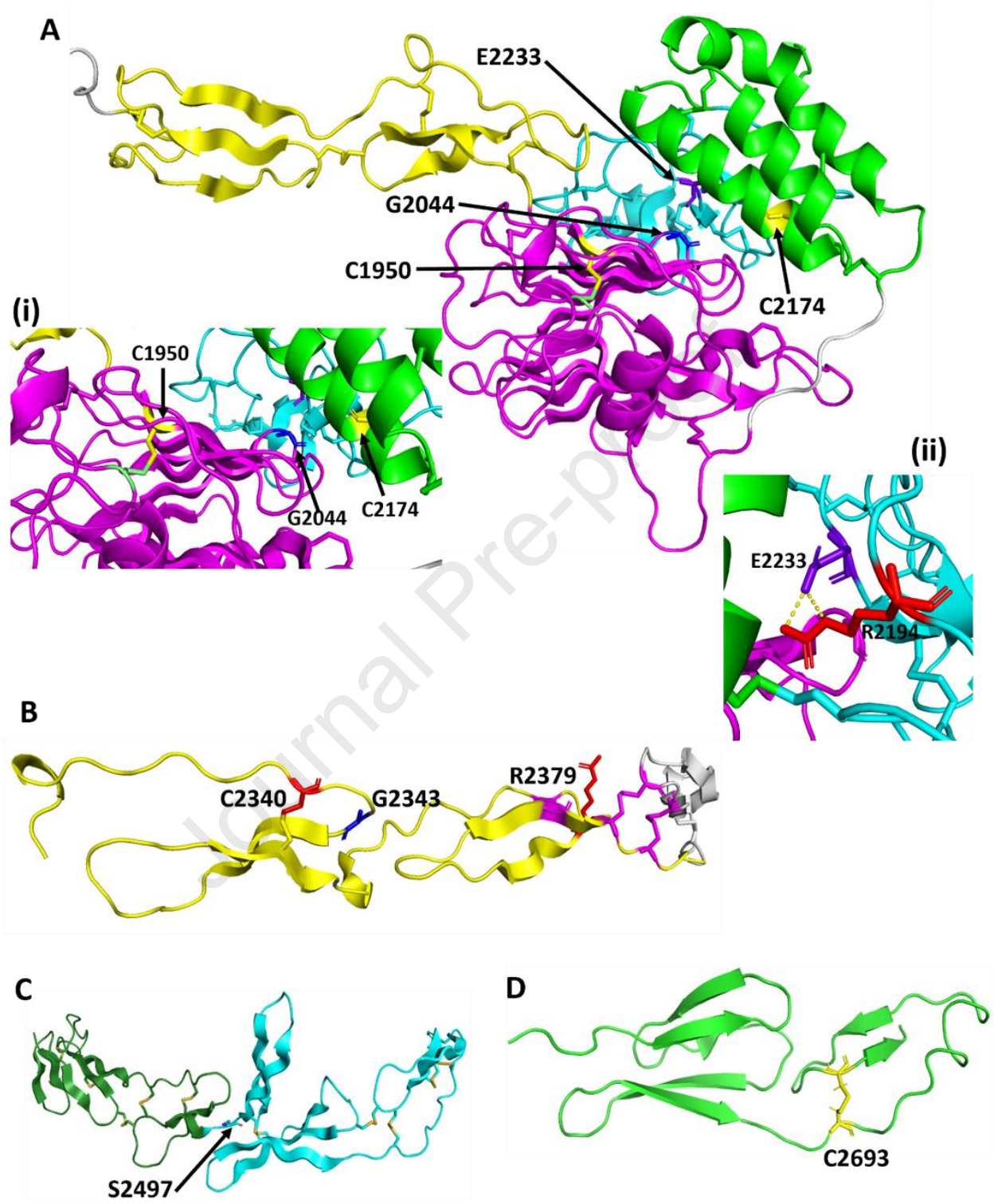

wtVWF
Cys1950Tyr
Gly2044Asp
Cys2174Gly
Glu2233Gln
Cys2340Tyr
Gly2343Val
Arg2379Cys
Ser2497Pro
Cys2693Tyr
DAPI
PDI
VWF
Merged
DAPI
PDI
VWF
Merged

Figure 5



Journal Pre-proof

Figure 6



Journal Pre-proof